

Astrophysical inputs on the SUSY dark matter annihilation detectability

F. Prada¹, A. Klypin², J. Flix³, M. Martínez³ and E. Simonneau⁴

¹ *Ramón y Cajal Fellow, Instituto de Astrofísica de Andalucía (CSIC), E-18008 Granada, Spain*

² *Department of Astronomy, New Mexico State University, Las Cruces NM 88003-8001, USA*

³ *Institut de Física D'Altes Energies, Universitat Autònoma, E-08193 Barcelona, Spain*

⁴ *Institut d'Astrophysique de Paris, CNRS, 75014 Paris, France*

(Dated: January 8, 2004)

If dark matter (DM), which is considered to constitute most of the mass of galaxies, is made of supersymmetric (SUSY) particles, the centers of galaxies should emit γ -rays produced by their self-annihilation. We present accurate estimates of continuum γ -ray fluxes due to neutralino annihilation in the central regions of the Milky Way. We use detailed models of our Galaxy, which satisfy available observational data, and include some important physical processes, which were previously neglected. Our models predict that spatially extended annihilation signal should be detected at high confidence levels by incoming experiments assuming that neutralinos make up most of the DM in the Universe and that they annihilate according to current SUSY models.

PACS numbers: 98.80.-k, 98.35.Ce, 98.35.Gi, 95.35.+d, 14.80.Ly

There is an increasing hope that the new generation of Imaging Atmospheric Čerenkov Telescopes (IACTs) would detect in the very near future the γ -ray signal coming from the annihilation products of the SUSY DM in galaxy halos (e.g., [1, 2, 3, 4]). The success of such a detection in competition with other indirect or direct experiments including accelerators will solve one of the most fundamental questions in Astrophysics and Particle Physics: the nature of the dark matter. The lightest supersymmetric particle (LSP) has been proposed to be a suitable candidate for the non-baryonic cold DM ([5, 6], see also [7, 8] for a review). The LSP is stable in SUSY models where R-parity is conserved [9, 10, 11] and its annihilation cross section and mass has the appropriate relic densities [8, 12] in the range allowed by WMAP, i.e. $0.095 < \Omega_{CDM} h^2 < 0.129$ [13]. We focus in the Minimal Supersymmetric extension of the Standard Model of particle physics (MSSM) where the LSP is the neutralino (χ). New upper limits on the neutralino mass (m_χ) have been estimated due to the constraints on the neutralino relic densities $\Omega_\chi h^2$ provided by WMAP; $m_\chi < 1500$ GeV based on the MSSM including minimal supergravity (mSUGRA) [12, 14]. A lower limit of $m_\chi \sim 100$ GeV has been set by the accelerators [15].

The number of neutralino annihilations in galaxy halos and therefore the expected gamma signal arriving at the Earth depends not only on the adopted SUSY model but also strongly depends on the DM density $\rho_{dm}(r)$. This is why the central region $r < 200$ pc of the Milky Way, where the density is the largest, is the favorite site to search for this signal. The expected total number of continuum γ -ray photons received per unit time and per unit area, from a circular aperture on the sky of width σ_t (the resolution of the telescope) observing at a given direction Ψ_0 relative to the center of the Milky Way can be written as:

$$F(E > E_{th}) = \frac{1}{4\pi} \text{YSUS} \cdot U(\Psi_0), \quad (1)$$

$$\text{YSUS} = \frac{N_\gamma \langle \sigma v \rangle}{2m_\chi^2}, \quad U(\Psi_0) = \int J(\Psi) B(\Omega) d\Omega,$$

where the factor YSUS (back-spelled SUSY) depends only on the physics of annihilating particles and all the astrophysical properties (such as the DM distribution and geometry considerations) appear only in the factor $U(\Psi_0)$. This factor also accounts for the beam smearing, where $J(\Psi) = \int_{l.o.s} \rho_{dm}^2(r) dl$, $dl = \pm r dr / \sqrt{r^2 - d_\odot^2 \sin^2 \Psi}$, is the integral of the line-of-sight of the square of the DM density along the direction Ψ , and $B(\Omega) d\Omega$ is the Gaussian beam of the telescope:

$$B(\Omega) d\Omega = \exp \left[-\frac{\theta^2}{2\sigma_t^2} \right] \sin \theta d\theta d\varphi. \quad (2)$$

The angles θ and φ are related with the direction of observation Ψ_0 and the line-of-sight angle Ψ by $\cos \Psi = \cos \Psi_0 \cos \theta + \sin \Psi_0 \sin \theta \cos \varphi$. We have assumed spherical symmetry for the DM particles around the Galactic Center and that the observer is located in the Galactic equatorial plane at a distance d_\odot (here 8.0 kpc).

The factor $\text{YSUS}/4\pi$ represents the isotropic probability of γ -ray production per unit of DM density. It can be determined for any SUSY model given the neutralino mass m_χ , the number of continuum γ -ray photons N_γ emitted per annihilation, with energy above the IACT energy threshold (E_{th}), and the thermally average cross section $\langle \sigma v \rangle$ of the DM particles. We can then estimate a YSUS parameter range, given a neutralino mass interval of $100 - 1500$ GeV, and a cross section $\langle \sigma v \rangle$ interval of $5 \times 10^{-27} - 3 \times 10^{-26} \text{ cm}^3 \text{ s}^{-1}$ obtained for a sample of MSSM models computed in [4, 21] with relic densities in agreement with the WMAP constraints. The number of continuum gamma photons produced per annihilation N_γ is obtained by integrating the continuum spectrum given by the decay of π^0 mesons produced in the fragmentation of quarks. It can be well approximated by the eq.(18) in [3], i.e.

$N_\gamma = 5/6 x^{3/2} - 10/3 x + 5\sqrt{x} + 5/(6\sqrt{x}) - 10/3$, where $x \equiv E_{th}/m_\chi$. This gives values of the YSUS parameter in the range of 10^{-34} to 10^{-30} photons $\text{GeV}^{-2} \text{cm}^3 \text{s}^{-1}$ for E_{th} from 1 to 400 GeV.

A cuspy DM halo $\rho_{dm}(r) \propto r^{-\alpha}$ predicted by the simulations of the Cold Dark Matter with the cosmological constant (Λ CDM) is often assumed for the calculations of $U(\Psi_0)$ (e.g., [1, 2, 3, 4, 16, 17, 18, 19, 20, 21, 22]). Cosmological N -body simulations indicate that the distribution of DM in relaxed halos varies between two shapes: the NFW [23] density profile $\rho(r) = \rho_0/x(1+x)^2$, $x \equiv r/r_s$ with asymptotic slope $\alpha = 1$ and the steeper Moore et al. [24] profile $\rho(r) = \rho_0/x^{1.5}(1+x)^{1.5}$, $\alpha = 1.5$. The density of DM also depends on two parameters of the approximations: the virial mass M_{vir} and the concentration $C \equiv r_{vir}/r_s$, where r_s is the characteristic radius of assumed approximation. For Milky Way-size halos the average concentration $C = 15$ and the 1σ -variance is $\Delta \log(C) = 0.11$. For Moore et al profile we define concentration as $C_{moore} = C_{NFW} * 1.72$.

Milky Way mass models with adiabatic compression.— The predictions for the DM halos are valid *only* for halos without baryons. When normal gas (“baryons”) loses its energy through radiative processes, it falls to the central region of forming galaxy. As the result of this redistribution of mass, the gravitational potential in the center changes substantially. The dark matter must react to this deeper potential by moving closer to the center and increasing its density. This increase in the DM density is often treated using adiabatic invariants. This is justified because there is a limit to the time-scale of changes in the mass distribution: changes of the potential at a given radius cannot happen faster than the dynamical time-scale defined by the mass inside the radius. Adiabatic contraction of dark matter in a collapsing protogalaxy was used already in 1962 [25]. In 1980, Zeldovich et al. [26] used it to set constraints of properties of elementary particles (annihilating massive neutrinos). They were also the first to present analytical expression for adiabatic compression (for pure radial orbits) and to make numerical tests to confirm that the mechanism works. The present form of analytical approximation (circular orbits) was introduced in [27]. If $M_{in}(r_{in})$ is the initial distribution of mass (the one predicted by cosmological simulations), then the final (after compression and formation of galaxy) mass distribution is given by $M_{fin}(r)r = M_{in}(r_{in})r_{in}$, where $M_{fin} = M_{DM} + M_{bar}$. This approximation was tested in numerical simulations [28, 29]. The approximation assumes that orbits are circular and, thus $M(r)$ is the mass inside the orbit. This is not true for elongated orbits: mass $M(r)$ is smaller than the real mass, which a particle “feels” when it travels along elongated trajectory. This difference in masses requires a relatively small correction: mass M should be replaced by the mass inside time-averaged radius of trajectories passing through given radius r : $M_{fin}(\langle r \rangle)r = M_{in}(\langle r_{in} \rangle)r_{in}$. We find the correction using Monte Carlo realizations of trajectories in the NFW equilibrium halo and finding the time-averaged

TABLE I: Models and constraints for the Milky Way Galaxy

	Model A NFW	Model B Moore et al.	Constr.
Virial mass, $10^{12} M_\odot$	1.07	1.14	—
Virial radius, kpc	264	270	—
Halo concentration C	11	12	10.3-21.5 (1.5σ)
Disk mass, $10^{10} M_\odot$	3.7	4.0	—
Disk scale length, kpc	3.2	3.5	2.5-3.5
Bulge mass, $10^9 M_\odot$	8.0	8.0	—
Black Hole mass, $10^6 M_\odot$	2.6	2.6	2.6
$M(< 100 \text{ kpc})$, $10^{11} M_\odot$	6.25	5.8	7.5 ± 2.5
Σ_{total} , $ z < 1.1 \text{ kpc}$ at R_\odot , $M_\odot \text{pc}^{-2}$	65	70	71 ± 6
Σ_{baryon} at R_\odot , $M_\odot \text{pc}^{-2}$	47	53	48 ± 8
V_{circ} at 3 kpc, km/s	203	205	200 ± 5

radii $\langle x \rangle \approx 1.72x^{0.82}/(1+5x)^{0.085}$, $x \equiv r/r_s$. This approximation predicts smaller contraction in the central regions, where individual trajectories are very elongated. It gives better fits than the standard approximation when compared with realistic cosmological simulations [30].

In order to make realistic predictions for annihilation rates, we construct two detailed models of the Milky Way Galaxy by redoing the full analysis of numerous observational data collected in [31]. The models are compatible with the available observational data for the Milky Way and their main parameters are given in Table I. More details on the model ingredients and the existing observational constraints can be found in [31]. Fig. 1 presents the distribution of mass and density in the models. While all observations were included, some of them are more important than others. The solar neighborhood is relatively well studied and, thus, provides important observational constraints. In Table I we present two local parameters: the total density of matter inside 1.1 kpc Σ_{total} (obtained from kinematics of stars) and the surface density of gas and stellar components Σ_{baryon} . Circular velocity V_{circ} at 3 kpc distance from the center provides another crucial constraint on models as emphasized in [32]. It is difficult to estimate errors of this parameter because of uncertain contribution of the galactic bar. We use $\pm 5 \text{ km/s}$ error, which is realistic, but it can be even twice larger. Probably the most debated constraint is coming from counts of microlensing events in the direction of the galactic bulge. Our models are expected to have the optical depth of microlensing events $\tau = 1.2 - 1.6 \times 10^{-6}$ and, thus, they are compatible with the values of τ determined recently from the observations $\tau = 1 - 1.5 \times 10^{-6}$ [33], but are excluded if $\tau > 2 \times 10^{-6}$ (see [31] for a detailed discussion on the bulge optical depth in our models).

Gamma-ray annihilation observability in the Milky Way.— The expected neutralino annihilation gamma flux, in units of YSUS/ 10^{-32} , can be computed from Eq. 1 for the compressed DM density profile provided by our Milky Way models as a function of the angular distance Ψ_0 from the Galactic Center. In Fig. 2 we show the pre-

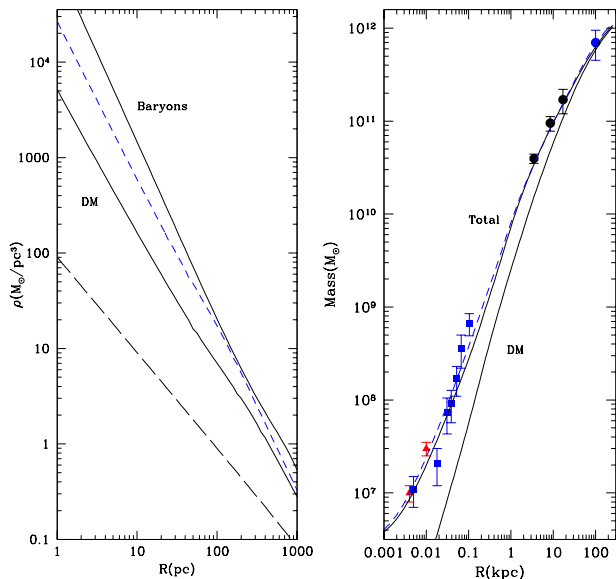


FIG. 1: Density and mass profiles for the Milky Way Galaxy. Symbols on right panel show observational constraints as taken from Klypin et al. [31]. The full and dashed curves labeled "Total" are total mass in NFW and Moore et al. models with adiabatic compression. DM mass in the NFW model is shown by the thick curve. In the central region most of the mass is in baryons. Left panel shows the density. The top full curve is the density of baryons. The dashed and full curves labeled "DM" are for the Moore et al. and NFW models with adiabatic compression. The long-dashed curve is the uncompressed NFW profile for comparison.

dicted fluxes. We also show as a comparison the expected flux for the uncompressed NFW density profile. The flux profiles were determined for a typical IACT of resolution $\sigma_t = 0.1^\circ$ and solid angle $\Delta\Omega = 10^{-5} \text{sr}$. We have multiplied the flux profiles by a factor of 1.7 quoted by Stoehr et al. [4] to account for the presence of substructure inside the Milky Way halo [34, 35].

The success of a detection requires that the minimum detectable gamma flux F_{\min} for an exposure of t seconds, given an IACT of effective area A_{eff} , angular resolution σ_t and threshold energy E_{th} exceeds a significant number M_s of standard deviations ($M_s\sigma$) the background noise $\sqrt{N_b}$, i.e. $F_{\min} A_{\text{eff}} t / \sqrt{N_b} \geq M_s$ (see, e.g., [1, 3]). The background counts (N_b) due to electronic and hadronic (cosmic protons and helium nuclei) cosmic ray showers have been estimated using the following expressions [1]: $N_e = 3 \times 10^{-2} E_{\text{th}}^{-2.3} t A_{\text{eff}} \Delta\Omega$, $N_h = 6.1 \times 10^{-3} E_{\text{th}}^{-1.7} t A_{\text{eff}} \Delta\Omega$. As an additional background, one has to consider also the contamination due to isolated muons which depending on the f.o.v. and altitude location of the telescope may be even the dominant background at some energy range (the "muon wall"). Preliminary studies [36] show that the muon background could be as relevant as the hadronic background at $E_{\text{th}} \gtrsim 100 \text{ GeV}$ while it can be effectively

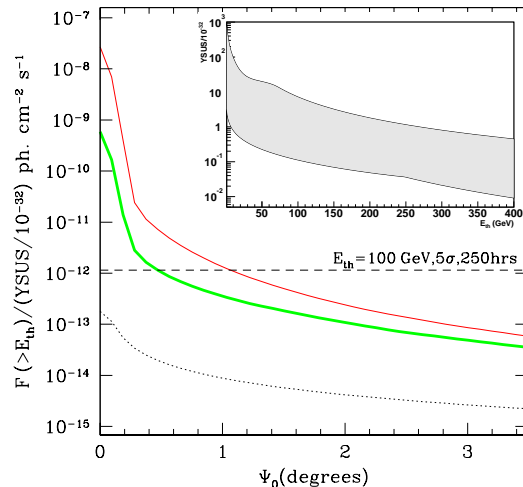


FIG. 2: Predicted continuum gamma flux as a function of distance Ψ_0 from the Galactic Center for Models A and B. The thick line shows the flux for the compressed NFW DM density profile of the Model A and the thin line for the compressed Moore et al. profile of the Model B. The flux profile for the uncompressed NFW profile is also shown for comparison (dotted line). The dashed line give the minimum detectable gamma flux F_{\min} at 5σ level for exposure of 250 hours and $E_{\text{th}} = 100 \text{ GeV}$ for a typical IACT. The inserted panel shows the YSUS/ 10^{-32} dependence with the IACT E_{th} . For a given E_{th} , the shadow region scans all the m_χ , $\langle\sigma v\rangle$ and N_γ intervals (see text).

rejected at lower E_{th} . The diffuse galactic and extragalactic gamma radiation are negligible compare to this background. Gamma point-like sources within the f.o.v can be resolved and taken out a posteriori. The E_{th} of an IACT depends on the zenith angle of observation. The Galactic Center is visible at different zenith angles by all present IACTs (e.g. CANGAROO-III, H.E.S.S., MAGIC, VERITAS), but in the best case an E_{th} of about 100 GeV can be achieved. Nevertheless, future planned installations may reduce the E_{th} below 10 GeV. The A_{eff} is also sensible to the zenith angle of observation, here we choose a value of $1 \times 10^9 \text{ cm}^2$. This detectability condition will allow us to compute the 5σ minimum detectable flux F_{\min} in 250 hours of integration with a typical IACT of $A_{\text{eff}} = 1 \times 10^9 \text{ cm}^2$ and $E_{\text{th}} = 100 \text{ GeV}$ (dashed line in Fig. 2). At a given distance from the Galactic Center only the flux values, for a particular model of the Milky Way, greater than F_{\min} will be detected. The detection will be much harder and may result only in a central spot in the case of an IACT with higher E_{th} , as the YSUS parameter declines with E_{th} (see Fig. 2).

The Milky Way models presented here include adiabatic compression and likely will result in a detection of the annihilation signal no matter what was the initial

(uncompressed) DM density profile. For current experiments this detection will be successful only for the very central regions, less than $\sim 0.4^\circ$ in the case of the Model A and close to $\sim 1^\circ$ in the case of the Model B. The compressed Moore et al. DM profile will provide a more extended gamma flux profile. The uncompressed NFW DM profile of the Model A will not be detected even in the direction of the Galactic Center. On the other hand, even the uncompressed Moore et al. profile of the Model B will give a positive detection in the very inner regions of the Milky Way.

The effect of the adiabatic compression included in our Milky Way mass models, which was previously ignored, is a crucial factor. It should be emphasized that for the central $\sim 3\text{kpc}$ of the Milky Way, where the baryons dominate, it does not make sense to use the dark matter profiles provided by cosmological N-body simulations: the DM must fall into the deep potential well created by the collapsed baryons. Thus, the models presented here are not extreme: they are the starting point for realistic predictions of the annihilation fluxes. One can envision few mechanisms to reduce the effect of the compression.

Transfer of the angular momentum to the dark matter as suggested in [31] is an option. Yet, recent simulations of formation of bars indicate that it is difficult to arrange a significant transfer of the angular momentum to the dark matter. The DM density in the central few parsec can be reduced if the central black hole formed by spiraling and merging of two black holes [37]. It can also be changed (probably reduced) by scattering of DM particles by stars in the central 2 pc [38]. If this happens, the flux from the central 2 pc can be significantly reduced. Yet, it will only decrease the amplitude of the central spike. The signal from 0.4° still could be detected because it mostly comes from distances 30-50 pc, which are much less affected by the uncertain physics around the black hole.

Acknowledgments

We acknowledge support of NASA and NSF grants to NMSU. We thank J. Primack, O. Gnedin, J. Betancort, A. Tasitsiomi and W. Wittek for discussions.

-
- [1] L. Bergström, P. Ullio, and J.H. Buckley, *Astropart. Phys.* 9, 137 (1998).
 - [2] E.A. Baltz, C. Briot, P. Salati, R. Taillet, and J. Silk, *Phys. Rev. D* 61, 23514 (2000).
 - [3] A. Tasitsiomi, and A.V. Olinto, *Phys. Rev. D* 66, 83006 (2002).
 - [4] F. Stoehr, S.D.M. White, V. Springel, G. Tormen, and N. Yoshida, *MNRAS*, 345, 1313 (2003).
 - [5] H. Goldberg, *Phys. Rev. Lett.* 50, 1419 (1983).
 - [6] J. Ellis, J.S. Hagelin, D.V. Nanopoulos, K. Olive, and M. Srednicki, *Nucl. Phys. B* 238, 453 (1984).
 - [7] J.R. Primack and D. Sacket, *Ann. Rev. Rev. Nucl. Part. Sci.* 38, 751 (1988).
 - [8] G. Jungman, M. Kamionkowski, and K. Griest, *Phys. Rep.* 267, 195 (1996).
 - [9] S. Weinberg, *Phys. Rev. D* 26, 287 (1982).
 - [10] L.J. Hall, and M. Suzuki, *Nucl. Phys. B* 231, 419 (1984).
 - [11] B.C. Allanach, A. Dedes, and H.K. Dreiner, *Phys. Rev. D* 60, 75014 (1999).
 - [12] J. Edsjo, M. Schelke, P. Ullio, and P. Gondolo, *hep-ph/0301106* (2003).
 - [13] D.N. Spergel et al., *Astrophys. J. Supp. Series*, 148, 175 (2003).
 - [14] J. Ellis, K.A. Olive, Y. Santoso, and V.C. Spanos, *Phys. Lett. B* 565, 176 (2003).
 - [15] Hagiwara, K. et al. (Particle Data Group), *Phys. Rev. D* 66, 10001 (2002).
 - [16] L. Bergström, J. Edsjö, P. Gondolo, and P. Ullio, *Phys. Rev. D* 59, 43506 (1999).
 - [17] C. Calcáneo-Roldán, and B. Moore, *Phys. Rev. D* 62, 123005 (2000).
 - [18] P. Ullio, L. Bergström, J. Edsjö, and C. Lacey, *Phys. Rev. D* 66, 123502 (2002).
 - [19] D. Hooper and B. Dingus, proceedings of the 34th COSPAR Scientific Assembly, *astro-ph/0212509* (2002).
 - [20] J.E. Taylor, and J. Silk, *MNRAS*, 339, 505 (2003).
 - [21] A. Tasitsiomi, J. Gaskins, and A.V. Olinto, *astro-ph/0307375* (2003).
 - [22] N.W. Evans, F. Ferrer, and S. Sarkar, *astro-ph/0311145* (2003).
 - [23] J.F. Navarro, C.S. Frenk, and S.D.M. White, *Astrophys. J.*, 490, 493 (1997).
 - [24] B. Moore, F. Governato, T. Quinn, J. Stadel, and G. Lake, *Astrophys. J. Lett.*, 499, L5 (1998).
 - [25] O.J. Eggen, D. Lynden-Bell, and A.R. Sandage, *Astrophys. J.*, 136, 748 (1962).
 - [26] Ya.B. Zeldovich, A.A. Klypin, M.Yu. Khlopov, and V.M. Chechetkin, *Soviet J. Nucl. Phys.*, 31, 664 (1980).
 - [27] G.R. Blumenthal, S.M. Faber, R. Flores and J.R. Primack, *Astrophys. J.*, 301, 27 (1986).
 - [28] J. Barnes, and S.D.M. White, *MNRAS*, 211, 753 (1984).
 - [29] R. Jesseit, N. Thorsten, A. Burkert, *Astrophys. J. Lett.*, 571, L89 (2002).
 - [30] A.V. Kravtsov, private communication (2004).
 - [31] A. Klypin, H. Zhao, and R.S. Somerville, *Astrophys. J.*, 573, 597 (2002).
 - [32] J. Binney and N.W. Evans, *MNRAS*, 327, L27 (2001).
 - [33] Afonso et al. for the EROS collaboration, *Astron. Astrophys.*, 404, 145 (2003); Popowski et al. for the MACHO collaboration, *astro-ph/0304464* (2003).
 - [34] A. Klypin, A.V. Kravtsov, O. Valenzuela, and F. Prada, *Astrophys. J.*, 522, 82 (1999).
 - [35] B. Moore, S. Ghigna, F. Governato, G. Lake, T. Quinn, J. Stadel, and P. Tozzi, *Astrophys. J. Lett.* 524, L19 (1999).
 - [36] M. Martínez, M. Mariotti, R. Mirzoyan for the MAGIC collaboration, in preparation (2004)
 - [37] P. Ullio, H.S. Zhao, and M. Kamionkowski, *Phys. Rev. D* 64, 043504 (2001).
 - [38] O. Gnedin, and J. Primack, *astro-ph/0308385* (2003)